

Supplementary Information

Designing highly tunable laminin inspired bioactive peptide hydrogel based biomaterials for directing cellular response

Ranit Bhandary ^a, Sourav Sen ^a, Sweta Mohanty ^a and Sangita Roy ^{a*}

^a Institute of Nano Science and Technology (INST), Sector 81, Knowledge City, Mohali
140306, Punjab, India

*Email: sangita@inst.ac.in

Table of contents

Table S1: LC-MS analysis data of the peptide from Chemdraw (Ultra 12.0) and ESI-MS.

Table S2: Gelation behavior of the laminin-inspired peptide by co-solvent approach using 5% DMSO with different peptide concentration.

Table S3: LC-MS analysis data of the scrambled peptide from Chemdraw (Ultra 12.0) and ESI-MS.

Table S4: Gelation behavior of the scrambled peptide sequence by co-solvent approach using 5% DMSO with different peptide concentration.

Table S5: Table of fiber diameter of the peptide hydrogels prepared at different concentrations.

Table S6: Water contact angle (WCA) values at different time points for the peptide hydrogels of different concentrations.

Table S7: The values of cell shape index (CSI) and area covered by fibroblast cells on control as well as peptide hydrogel scaffold as determined by F-actin staining.

Table S8: The values of cell shape index (CSI) and area covered by neuronal cells on control as well as peptide hydrogel scaffold as determined by β -tubulin staining.

Figure S1: Reverse phase HPLC chromatogram of Nap-IVVSIVNGR.

Figure S2: LC-MS spectra of laminin inspired peptide sequence analyzed using ESI-MS technique.

Figure S3: FTIR spectra of 25 mM Nap-IVVSIVNGR hydrogels (prepared in 5% DMSO/water) after solvent exchange showing diminished sulfoxide peak at 1020 cm^{-1} .

Figure S4: LC-MS spectra of scrambled peptide analyzed using ESI-MS technique.

Figure S5: Reverse phase HPLC chromatogram of scrambled peptide sequence Nap-SVGRINVIV.

Figure S6: CD spectra of scrambled peptide hydrogel at different concentrations.

Figure S7: Comparison of the CD spectra of a) Nap-IVVSIVNGR and b) Nap-SVGRINVIV (scrambled peptide) at different concentration.

Figure S8: FTIR spectra of Nap-IVVSIVNGR peptide monomer powder along with freeze dried peptide hydrogels prepared at different concentrations.

Figure S9: Secondary structure evaluation of the scrambled hydrogels at different peptide concentrations by various spectroscopic techniques: (a) FTIR- spectroscopic measurement, (b) ThT binding assay.

Figure S10: Representative fluorescence emission spectra of peptide amphiphile in sol and gel states, indicating self-assembly by the quenched monomeric emission of the naphthoxy group in the gel state.

Figure S11: a) Tht binding assay and b) Congo red binding study of the peptide hydrogels at different concentrations.

Figure S12: Fluorescence microscopic images of the ThT bound peptide hydrogels at different concentrations (a) ThT Control, (b) 20 mM, (c) 25 mM, and (d) 30 mM.

Figure S13: FESEM images of the peptide hydrogels at different peptide concentrations (a) 20 mM, (b) 25 mM, and (c) 30 mM Nap-IVVSIVNGR.

Figure S14: Morphological analysis of Nap-SVGRINVIV scrambled peptide hydrogels at different concentrations. TEM images of the gels prepared at: (a) 20 mM, (b) 25 mM, and (c) 30 mM of peptide concentration. Scale bar is 200 nm.

Figure S15: Morphological analysis of Nap-SVGRINVIV scrambled peptide hydrogels at different concentrations. FESEM images of the gels prepared at: (a) 20 mM, (b) 25 mM, and (c) 30 mM of peptide concentration. Scale bar is 100 nm.

Figure S16: Strain sweep analysis of laminin-inspired peptide hydrogels at different concentrations (a) 20 mM, (b) 25 mM, and (c) 30 mM.

Figure S17: Mechanical strength analysis of the scrambled hydrogels at different concentration using a frequency sweep experiment.

Figure S18: (a) Time-dependent variation in the water contact angle of Nap-IVVSIVNGR hydrogels. Images of the water droplets after landing on surfaces of 20 mM hydrogel at (b) 5 s, (c) 50s, 25 mM hydrogel at (d) 5 s, (e) 50 s, 30 mM hydrogel at (f) 5 s, (g) 50 s.

Figure S19: Determination of cellular viability of the scrambled peptide and comparison of cellular viability with the laminin inspired peptide Nap-IVVSIVNGR: Cellular viability of

hydrogel on (a) L929 cells, (b) SH-SY5Y cells, and (c) Bright field images of both the cells in control and after 24h following treatment with peptide at 0.88 mM concentration.

Figure S20: Cellular growth and proliferation study of the peptide at subgelation concentration on (a) L929 cells, (b) SH-SY5Y cells.

Figure S21: Cellular growth and proliferation study of the scrambled peptide hydrogels on (a) L929 cells, (b) SH-SY5Y cells.

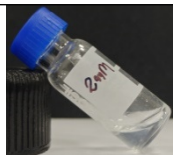
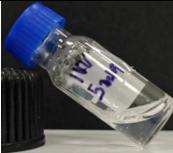

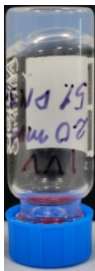
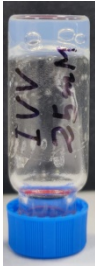
Figure S22: 3D stability study of the hydrogels in PBS having different peptide concentrations at different time points.

Figure S23: Confocal laser scanning microscopy images of SH-SY5Y cells in 3D cell culture conditions on (a) Control, (b) 20 mM Nap-IVVSIVNGR hydrogel, (c) 25 mM Nap-IVVSIVNGR hydrogel, (d) 30 mM Nap-IVVSIVNGR hydrogel. Scale bar is 200 μ m, Z-stack rendering images of the L929 cells after live/dead staining in the 3-D cell culture conditions in case of (e) Control, (f) 20 mM Nap-IVVSIVNGR hydrogel, (g) 25 mM Nap-IVVSIVNGR hydrogel, (h) 30 mM Nap-IVVSIVNGR hydrogel. The scale bar is 200 μ m.

Table S1: LC-MS analysis data of the peptide from Chemdraw (Ultra 12.0) and ESI-MS.

| Peptide Nap-IVVSIVNGR | Calculated molecular weight (Chem Draw Ultra 12.0) | Found m/z value (M+H) ⁺ (ESI -MS) |
|---|--|--|
| C ₅₄ H ₈₆ N ₁₄ O ₁₃ | 1139.37 | 1140.65 |

Table S2: Gelation behavior of the laminin-inspired peptide by co-solvent approach using 5% DMSO with different peptide concentration.

| Concentration of laminin-inspired peptide (mM) | Gelation time | Optical images of the gels formed at different concentrations. |
|--|---------------|---|
| 2 | No Gelation |  |
| 5 | No Gelation |  |
| 10 | No Gelation |  |
| 20 | 72 h |  |
| 25 | 48 h |  |

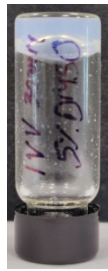

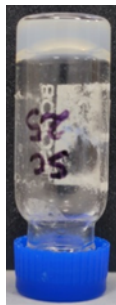
| | | |
|----|------|---|
| 30 | 24 h |  |
|----|------|---|

Table S3: LC-MS analysis data of the scrambled peptide from Chemdraw (Ultra 12.0) and ESI-MS.

| Peptide Nap-SVGRINVIV | Calculated molecular weight (Chem Draw Ultra 12.0) | Found m/z value (ESI -MS) | Found m/z value (M+H) ⁺¹ (ESI -MS) | Found m/z value (M+2H) ⁺² (ESI -MS) |
|---|--|---------------------------|---|--|
| C ₅₄ H ₈₆ N ₁₄ O ₁₃ | 1139.37 | 1137.65 | 1138.65 | 1139.66 |

Table S4: Gelation behavior of the scrambled peptide sequence by co-solvent approach using 5% DMSO with different peptide concentration.

| Concentration of scrambled peptide (mM) | Gelation time | Optical images of the gels formed at different concentrations. |
|---|---------------|---|
| 20 | 72 h |  |
| 25 | 48 h |  |


| | | |
|----|------|---|
| 30 | 24 h |  |
|----|------|---|

Table S5: Table displaying fiber diameter of the nanofibrous network of the peptide hydrogels prepared at different concentrations as revealed from TEM images.

| Concentration of Nap-IVVSIVNGR peptide (mM) | Fiber Diameter (nm) |
|---|---------------------|
| 20 | 10.46 ± 1.72 |
| 25 | 9.85 ± 1.15 |
| 30 | 8.16 ± 0.82 |

Table S6: Water contact angle (WCA) values at different time points for the peptide hydrogels of different concentrations.

| Time Points (Sec) | Water contact angle at different peptide concentration (°) | | |
|-------------------|--|-------|-------|
| | 20 mM | 25 mM | 30 mM |
| 5 | 32.29 | 34.57 | 30.91 |
| 10 | 31.26 | 30.40 | 26.05 |
| 20 | 29.64 | 27.08 | 24.64 |
| 30 | 29.75 | 25.62 | 24.15 |
| 40 | 29.74 | 23.81 | 23.38 |
| 50 | 28.30 | 23.48 | 22.85 |

Table S7: The values of cell shape index (CSI) and area covered by fibroblast cells on control as well as peptide hydrogel scaffold as determined by F-actin staining.

| Peptide Concentration (mM) | CSI Values | Area Covered (μm^2) |
|----------------------------|-----------------|----------------------------------|
| Control | 0.61 ± 0.05 | 309.58 ± 38.73 |
| 20 | 0.75 ± 0.07 | 273.60 ± 33.82 |
| 25 | 0.45 ± 0.03 | 312.35 ± 31.50 |
| 30 | 0.54 ± 0.05 | 389.13 ± 34.63 |

Table S8: The values of cell shape index (CSI) and area covered by neuronal cells on control as well as peptide hydrogel scaffold as determined by β -tubulin staining.

| Peptide Concentration (mM) | CSI Values | Area Covered (μm^2) |
|----------------------------|-----------------|----------------------------------|
| Control | 0.79 ± 0.05 | 267.93 ± 33.40 |
| 20 | 0.90 ± 0.03 | 194.39 ± 36.04 |
| 25 | 0.87 ± 0.05 | 292.93 ± 26.50 |
| 30 | 0.82 ± 0.02 | 349.69 ± 27.24 |

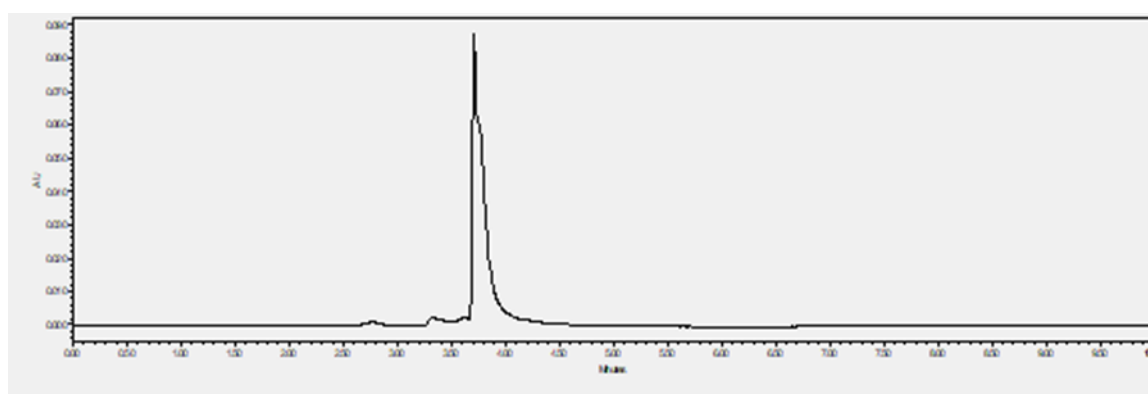


Figure S1: Reverse phase HPLC chromatogram of Nap-IVVSIVNGR.

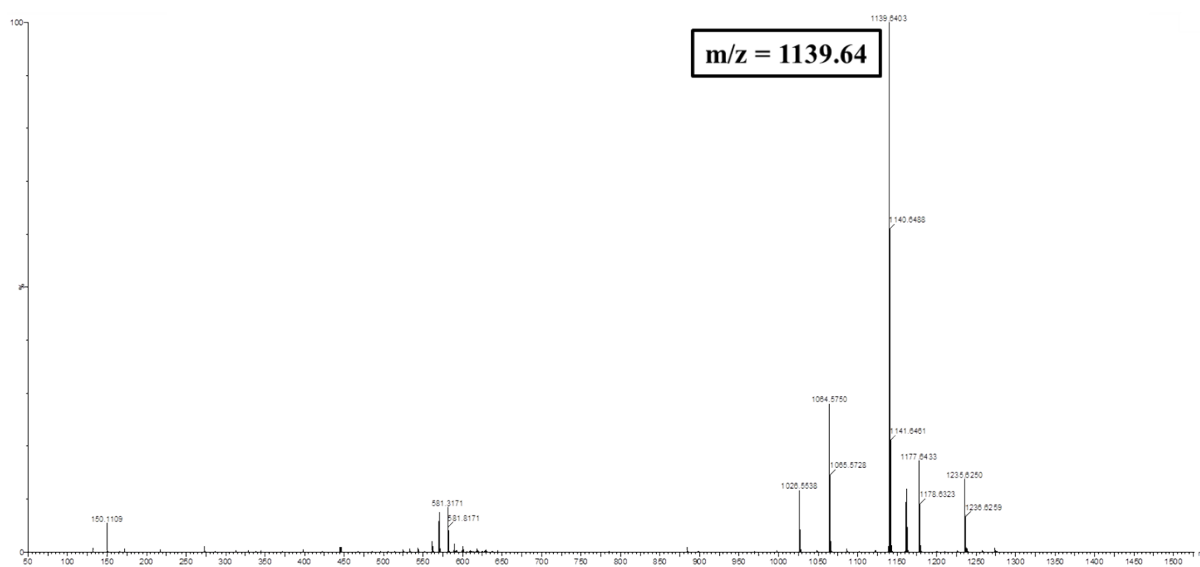


Figure S2: LC-MS spectra of laminin inspired peptide sequence analyzed using ESI-MS technique.

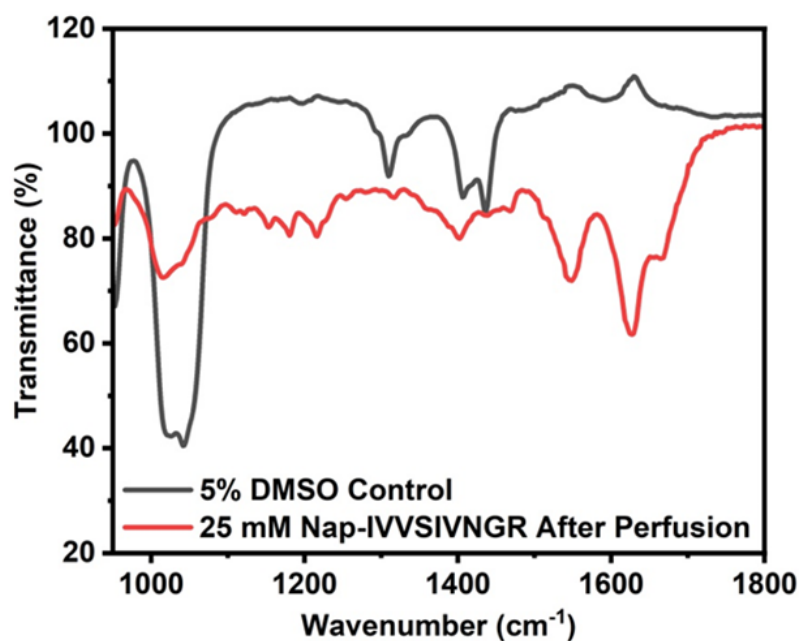


Figure S3: FTIR spectra of 25 mM Nap-IVVSIVNGR hydrogels (prepared in 5% DMSO/water) after solvent exchange showing diminished sulfoxide peak at 1020 cm⁻¹.

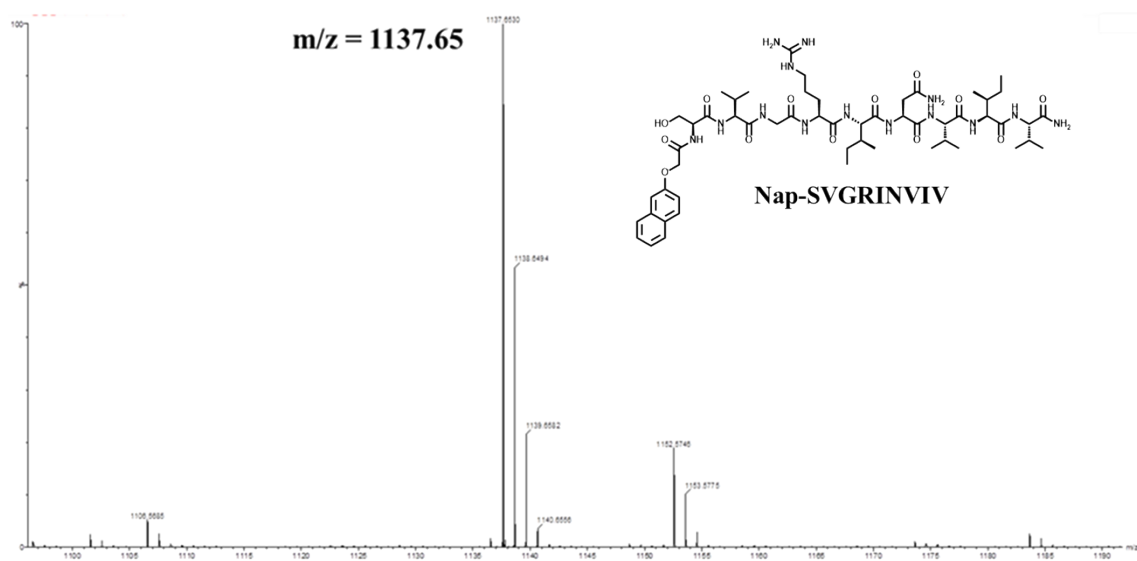


Figure S4: LC-MS spectra of scrambled peptide analyzed using ESI-MS technique.

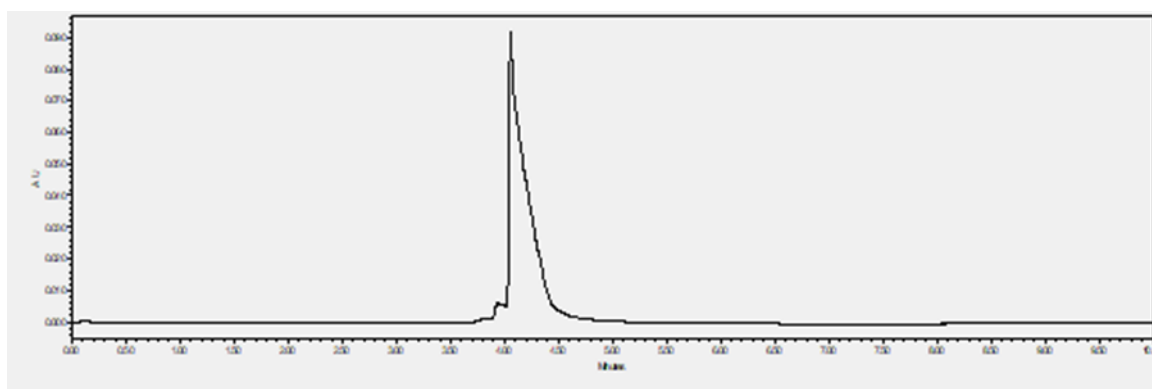


Figure S5: Reverse phase HPLC chromatogram of scrambled peptide sequence Nap-SVGRINVIV.

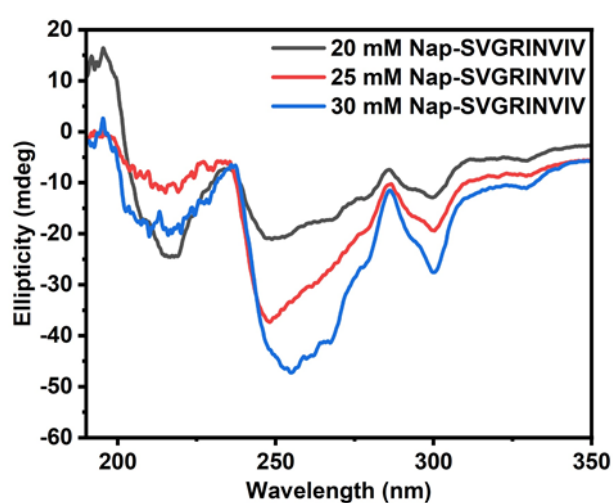


Figure S6: CD spectra of scrambled peptide hydrogel at different concentrations.

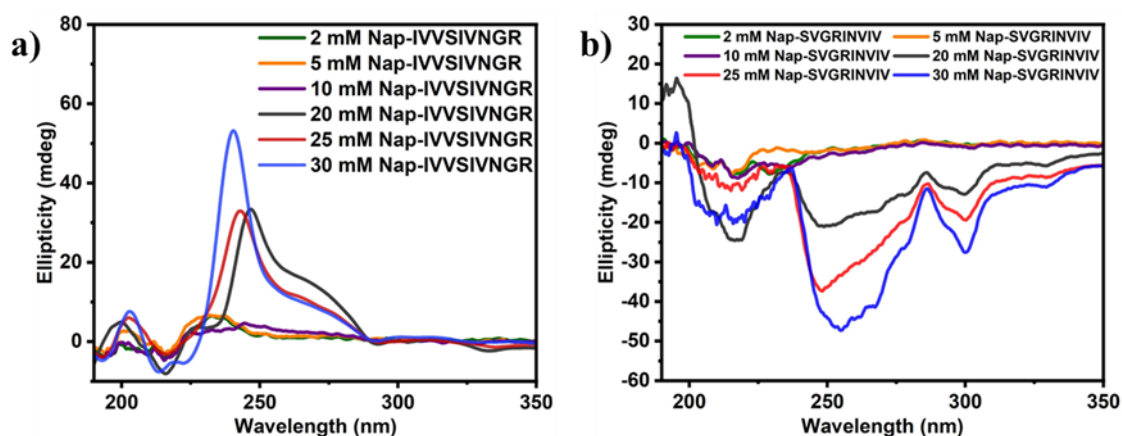


Figure S7: Comparison of the CD spectra of a) Nap-IVVSIVNGR and b) Nap-SVGRINVIV (scrambled peptide) at different concentration.

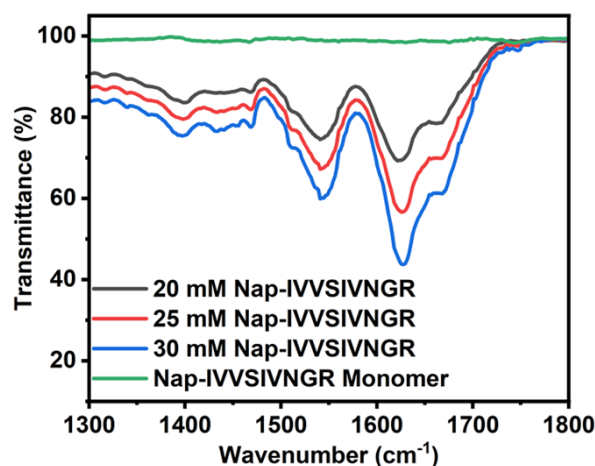


Figure S8: FTIR spectra of Nap-IVVSIVNGR peptide monomer powder along with freeze dried peptide hydrogels prepared at different concentrations.

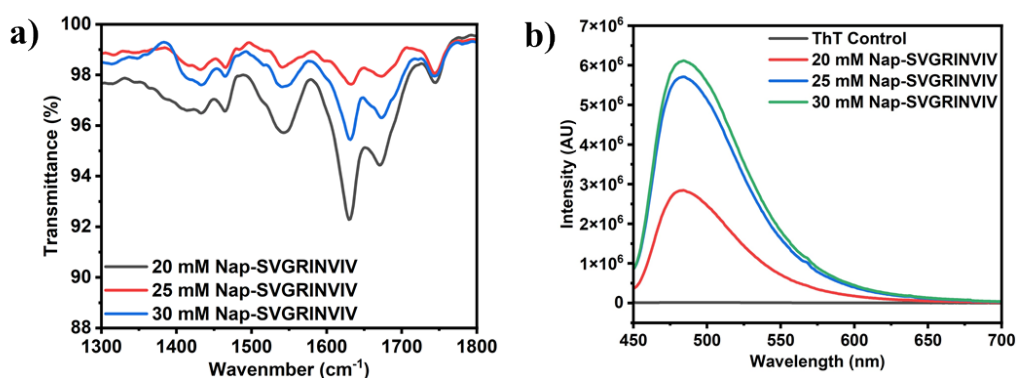


Figure S9: Secondary structure evaluation of the scrambled hydrogels at different peptide concentrations by various spectroscopic techniques: (a) FTIR- spectroscopic measurement, (b) ThT binding assay.

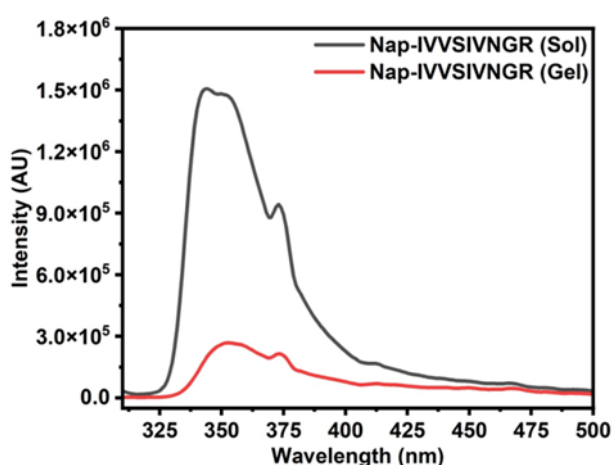


Figure S10: Representative fluorescence emission spectra of peptide amphiphile in sol and gel states, indicating self-assembly by the quenched monomeric emission of the naphthoxy group in the gel state.

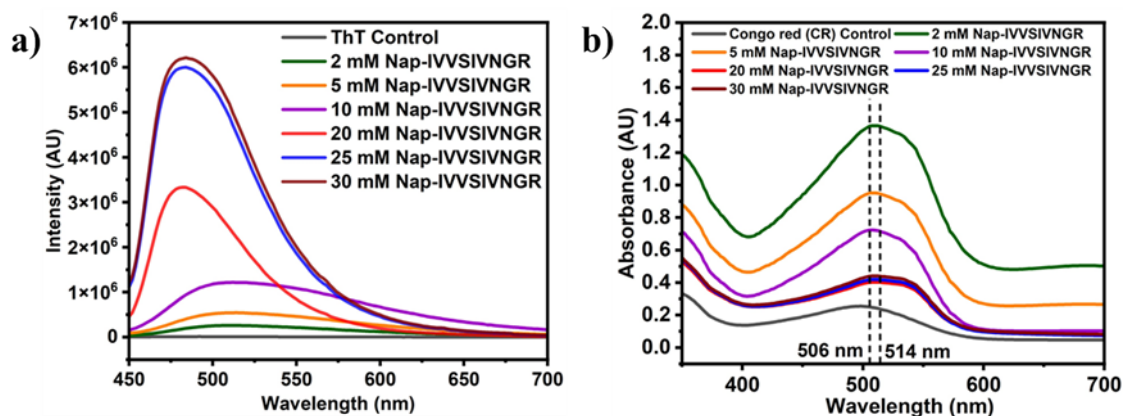


Figure S11: a) Tht binding assay and b) Congo red binding study of the peptide hydrogels at different concentrations.

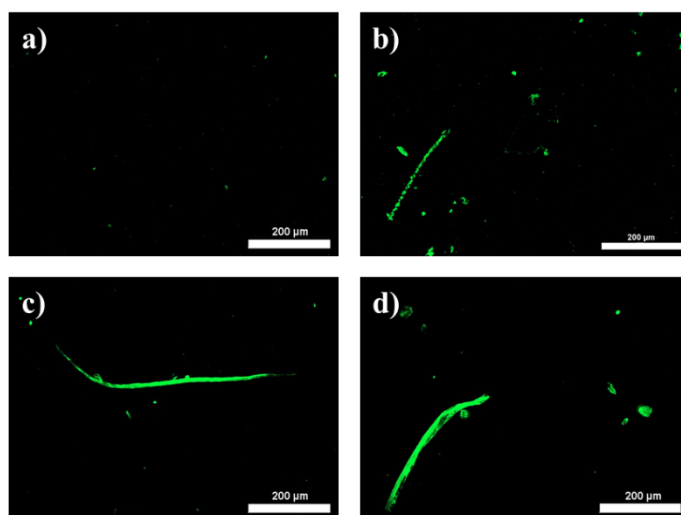


Figure S12: Fluorescence microscopic images of the ThT bound peptide hydrogels at different concentrations (a) ThT Control, (b) 20 mM, (c) 25 mM, and (d) 30 mM.

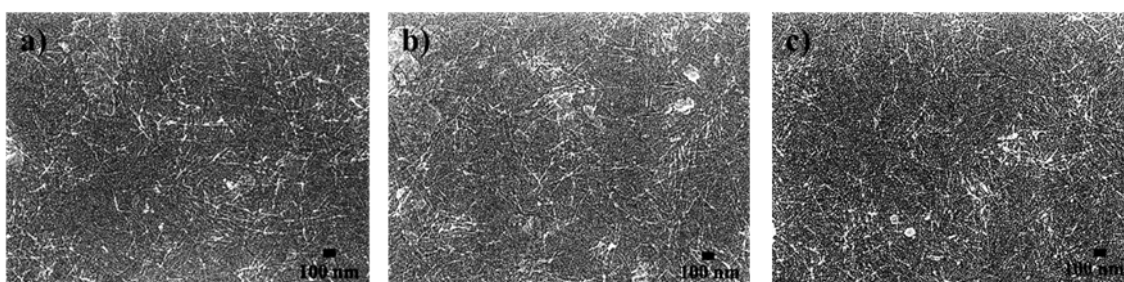


Figure S13: FESEM images of the peptide hydrogels at different peptide concentrations (a) 20 mM, (b) 25 mM, and (c) 30 mM Nap-IVVSIVNGR.

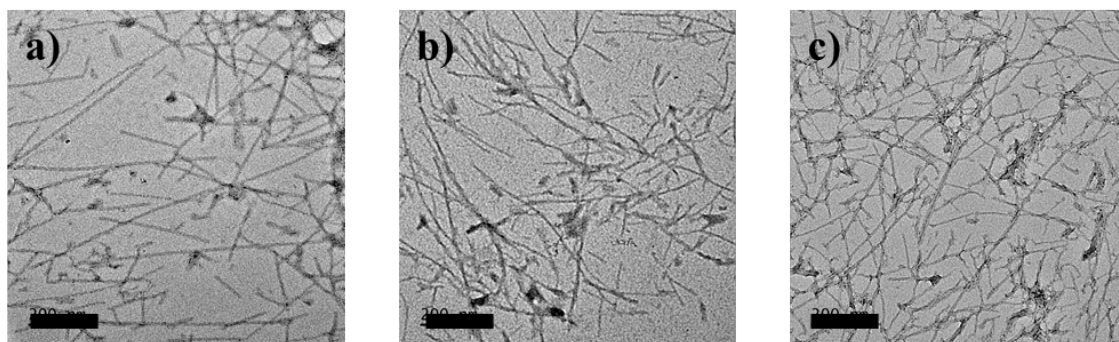


Figure S14: Morphological analysis of Nap-SVGRINVIV scrambled peptide hydrogels at different concentrations. TEM images of the gels prepared at: (a) 20 mM, (b) 25 mM, and (c) 30 mM of peptide concentration. Scale bar is 200 nm.

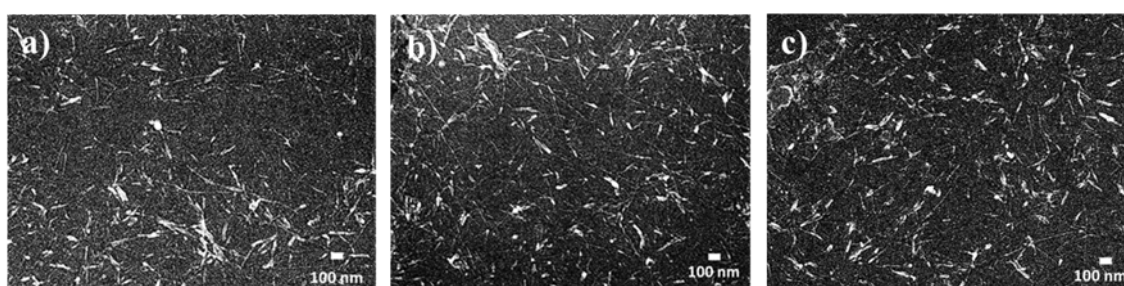


Figure S15: Morphological analysis of Nap-SVGRINVIV scrambled peptide hydrogels at different concentrations. FESEM images of the gels prepared at: (a) 20 mM, (b) 25 mM, and (c) 30 mM of peptide concentration. Scale bar is 100 nm.

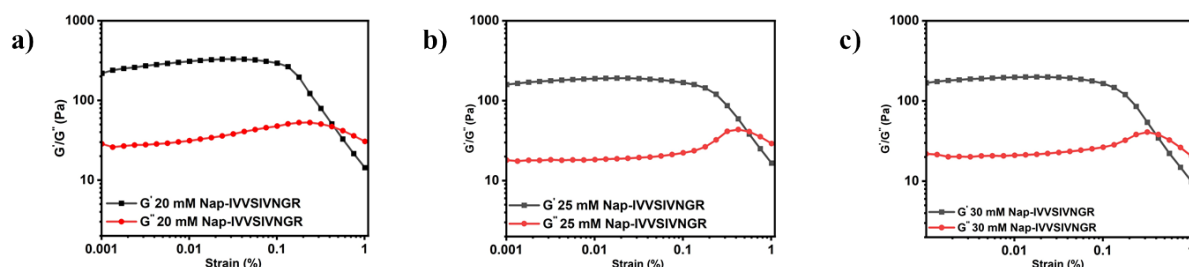


Figure S16: Strain sweep analysis of laminin-inspired peptide hydrogels at different concentrations (a) 20 mM, (b) 25 mM, and (c) 30 mM.

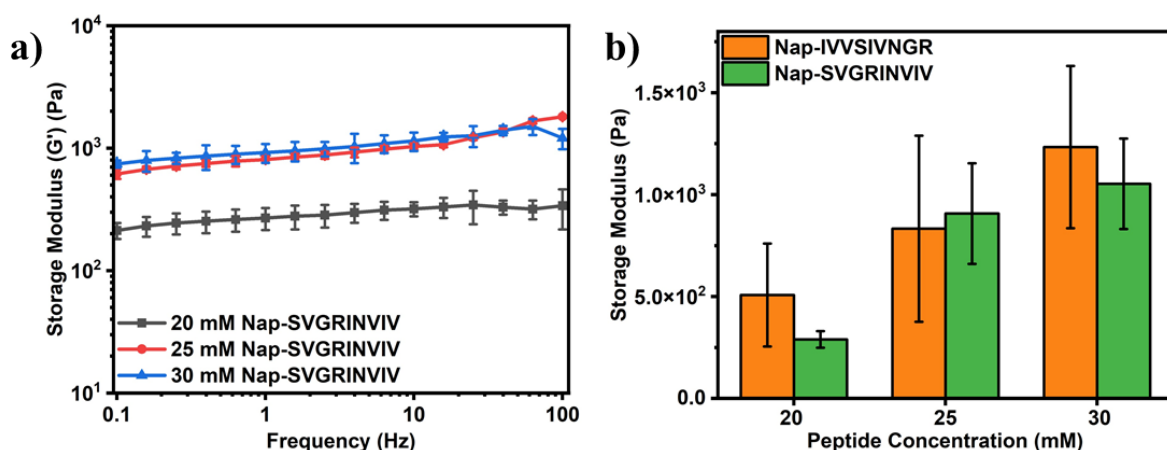


Figure S17: Mechanical strength analysis of the scrambled hydrogels at different concentration using a frequency sweep experiment.

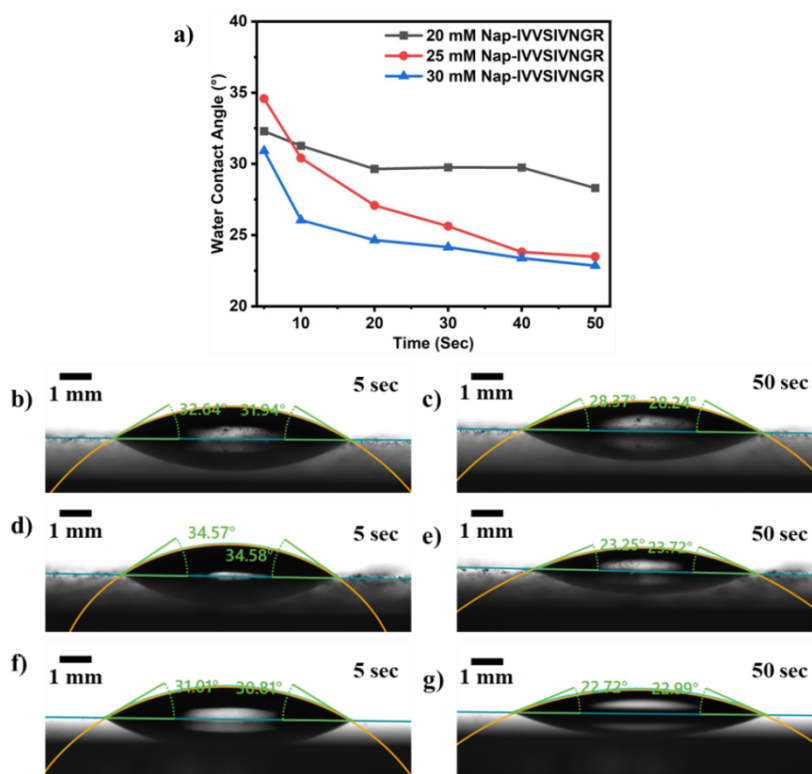


Figure S18: (a) Time-dependent variation in the water contact angle of Nap-IVVSIVNGR hydrogels. Images of the water droplets after landing on surfaces of 20 mM hydrogel at (b) 5 s, (c) 50s, 25 mM hydrogel at (d) 5 s, (e) 50 s, 30 mM hydrogel at (f) 5 s, (g) 50 s.

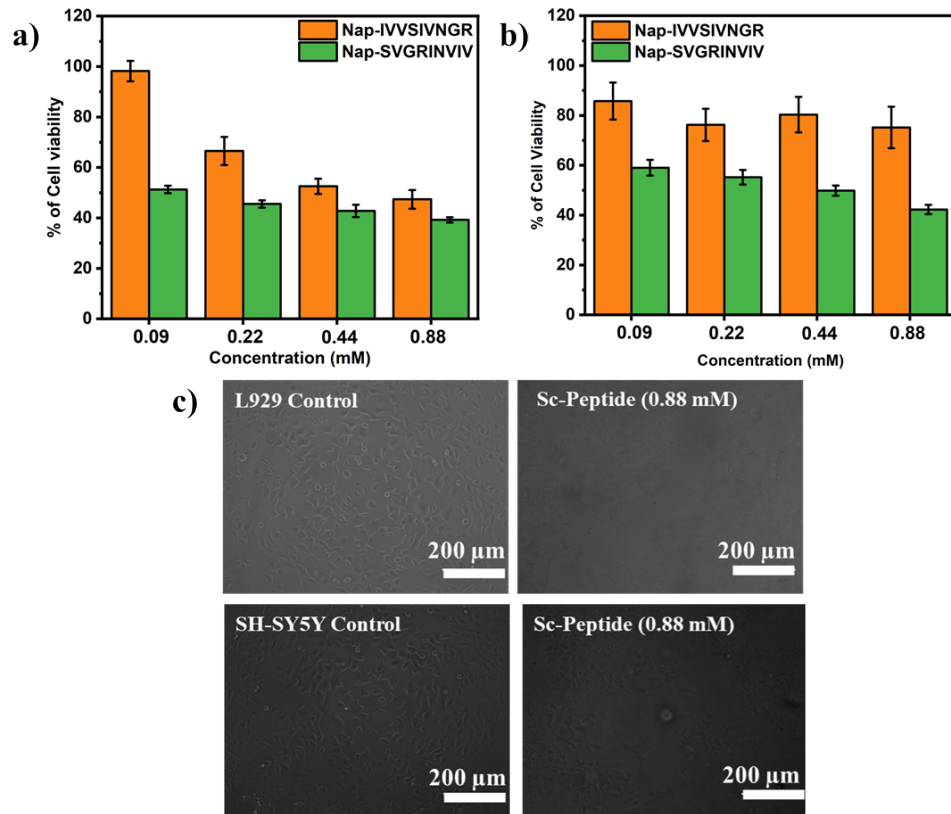


Figure S19: Determination of cellular viability of the scrambled peptide and comparison of cellular viability with the laminin inspired peptide Nap-IVVSIVNGR: Cellular viability of hydrogel on (a) L929 cells, (b) SH-SY5Y cells, and (c) Bright field images of both the cells in control and after 24h following treatment with peptide at 0.88 mM concentration.

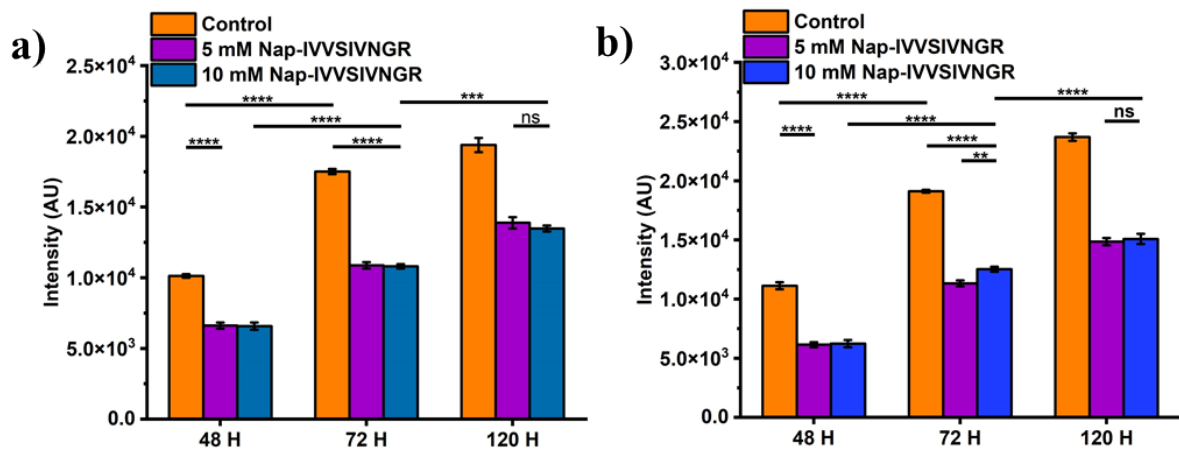


Figure S20: Cellular growth and proliferation study of the peptide at subgelation concentration on (a) L929 cells, (b) SH-SY5Y cells.

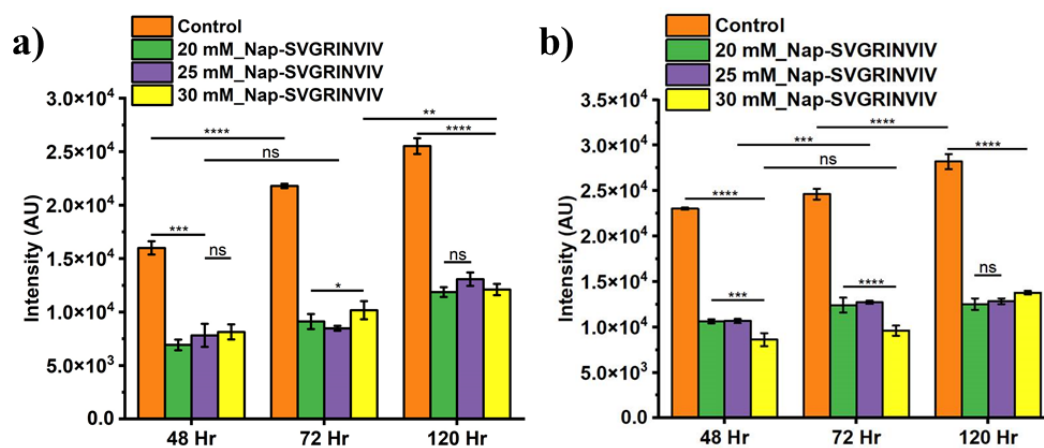


Figure S21: Cellular growth and proliferation study of the scrambled peptide hydrogels on (a) L929 cells, (b) SH-SY5Y cells.

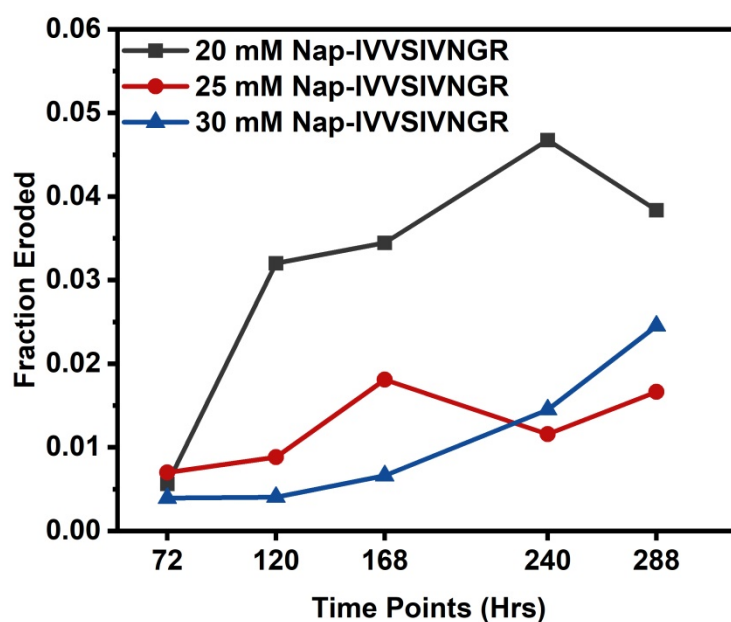


Figure S22: 3D stability study of the hydrogels in PBS having different peptide concentrations at different time points.

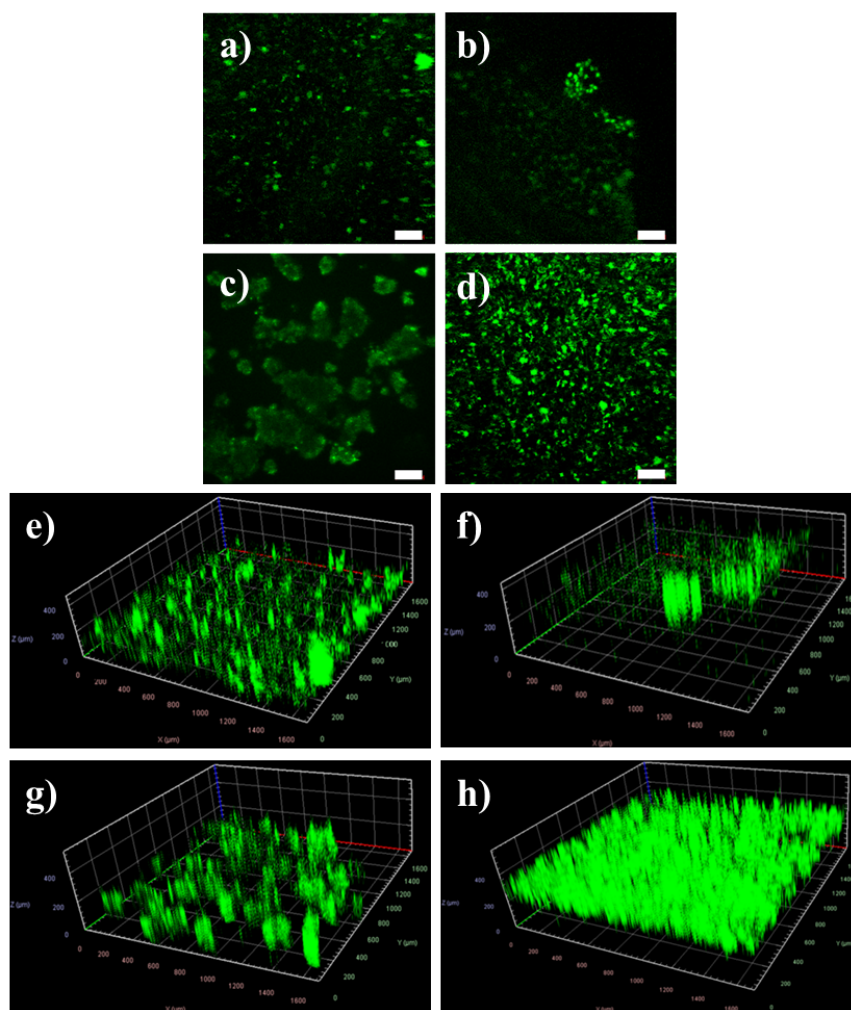


Figure S23: Confocal laser scanning microscopy images of SH-SY5Y cells in 3D cell culture conditions on (a) Control, (b) 20 mM Nap-IVVSIVNGR hydrogel, (c) 25 mM Nap-IVVSIVNGR hydrogel, (d) 30 mM Nap-IVVSIVNGR hydrogel. Scale bar is 200 μm, Z-stack rendering images of the L929 cells after live/dead staining in the 3-D cell culture conditions in case of (e) Control, (f) 20 mM Nap-IVVSIVNGR hydrogel, (g) 25 mM Nap-IVVSIVNGR hydrogel, (h) 30 mM Nap-IVVSIVNGR hydrogel. The scale bar is 200 μm.